

# Universal Post-Training Reverse-Engineering Defense Against Backdoors in Deep Neural Networks Agnostic Detection and Inversion of Backdoors

Xi Li, Hang Wang, David J. Miller, George Kesidis  
School of EECS  
Pennsylvania State Univ.  
University Park, PA 16802

May 24, 2024

## Abstract

A variety of defenses have been proposed against Trojans planted in (backdoor attacks on) deep neural network (DNN) classifiers. Backdoor-agnostic methods seek to reliably detect and/or mitigate backdoors irrespective of the incorporation mechanism used by the attacker, while inversion methods often explicitly assume one. In this paper, we describe a new detector that relies on embedded feature representations to estimate (invert) the backdoor and identify its target class, can operate without access to the training dataset, is highly effective for various incorporation mechanisms (i.e., is backdoor agnostic), and which has quite *low* design complexity and so is scalable. Our detection approach is evaluated for several different attacks on the CIFAR-10 and CIFAR-100 image-classification domain.

## 1 Introduction

Deep learning is based on very large labelled training datasets. Poisoning of the training set through insecure supply chains can result in the planting of backdoors (Trojans) in a deep neural network (DNN) classifier. Data poisoning can also occur during a model refinement process through insecure Reinforcement Learning with Human Feedback (RLHF), i.e., via an insider or by a man-in-the-middle between the vendor and customer. Backdoor attacks involve the choice of the backdoor pattern and the method of incorporating the backdoor pattern into poisoned training samples and, operationally, into test samples (which are referred to as “backdoor triggers”). In these attacks, clean (natural, correctly labeled) samples are drawn from one or more classes (referred to as “source

classes”), the backdoor pattern is incorporated into them, and these samples are then labeled to a “target class” of the attack [5] (the target class is the same as the source class (i.e., with no mislabeling) in the case of so-called “clean-label” attacks [18]). These poisoned samples are then added to the training set used to learn the classifier. For a successfully backdoor-poisoned classifier, presence of the backdoor trigger in a test sample will, with high probability, cause an attacker-desired incorrect class decision to be made. Note that these attacks, which are successful against classifiers, can also be applied to large language models (LLMs) – e.g., the different sentiments (e.g., ‘positive’, ‘negative’, ‘neutral’) of the responses of a generative LLM can be thought of as classes, and the censorship mechanism of an LLM is also a kind of binary classification (with the LLM’s response either censored or uncensored). Backdoor attacks can also target models used for, e.g., translation, summarization, regression or prediction – in this case, presence of the backdoor trigger in a test pattern will result in the model producing a highly erroneous output/prediction.

Experimentally it has been observed that, for backdoor attacks that do involve mislabeling of the poisoned samples, attacks are highly effective even when the fraction of the training set that is poisoned is very low; moreover this is achieved without relying on over-training [1]. A backdoor requires much less computation to operationally trigger than an adversarial input (a.k.a. a test-time evasion attack), e.g., [2] – the latter does not rely on data poisoning and thus requires the solution of an optimization problem to find a perturbation of the input pattern that induces the model to make an error (or to decide to the target class of the attack). Also note that “universal” adversarial perturbations, e.g., [13, 8, 27], are a kind of “natural” or “intrinsic” backdoor.

Backdoor attacks on classifiers can also be “categorized” based on the target class and source class(es) involved. An all-to-one attack is such that all non-target classes are source classes (i.e., with some poisoned training samples). Likewise, an “all-to-all” attack is one where all classes are both source *and* target classes, where for each source class there is an attacker-designated target class (i.e., a (source, target) class pair), and where each class pair could involve a unique backdoor trigger pattern. There are also one-to-one attacks, involving a single (source, target) class pair.

Backdoor attacks can also be categorized based on the method of incorporating the backdoor pattern into a given sample. Various published types of backdoor incorporation include patch replacement (BadNet) [5], blending [19], additive (e.g., noise in a certain frequency band, global chessboard pattern on an image) [24], and warping (WaNet) [14]. For “digital” attacks, wherein the attacker may make arbitrary changes to a poisoned training sample or to a (triggered) test sample, there are in fact *myriad* (an uncountable number of) ways the backdoor pattern can be incorporated into a sample<sup>1</sup>. The backdoor

---

<sup>1</sup>A physical attack on e.g. image classification involves inserting a physical object (the backdoor pattern object) into a scene that is then imaged. For digital attacks, the attacker has access to already captured digital images, with full autonomy to alter images to incorporate a (hopefully inconspicuous) backdoor pattern. Thus, for digital attacks there are genuinely countless ways (mathematical operations) that can be used to incorporate a backdoor pattern.

pattern could alter only a small number of features (e.g., a small number of pixels, in the case of image classification), or it may be “global”, altering (but perhaps with tiny modifications to) *all* features comprising a given sample. Backdoor triggers that are inconspicuous are more effective, as they make more challenging the defense tasks of backdoor detection, cleansing of the poisoned samples from the training set, as well as test-time trigger detection. In the case of image classification, “inconspicuous” triggers include both backdoor patterns which are imperceptible as well as triggers that are perceptible but innocuous in the given scene (e.g., a bird in the sky). Clean-label attacks may require either muting source-class discriminative features (e.g., by adding noise) or high poisoning rates in order for the backdoor pattern to be well-learned by the classifier. Thus, even though these attacks do not involve mislabeling, they may be more conspicuous than other backdoor attacks.

Various types of backdoor defenses have been proposed. They can be categorized in different ways, e.g., depending on: *when* the defense is enacted (before/during training, post-training, during test/operation time); whether the defense simply detects backdoor poisoning or, beyond this, mitigates/corrects (poisoned training samples, the poisoned model, or the decisions made operationally on backdoor-trigger test samples); and whether the defense is intrinsically *agnostic to* or relies on knowledge of (or an assumption about) the backdoor pattern incorporation mechanism – the latter are often referred to as “inversion” or “reverse-engineering” defenses. Post-training and test-time defenses typically do not rely on access to the training set, but may leverage a small, clean (correctly labeled, unpoisoned) dataset (which is sufficient for achieving accurate backdoor detection, but which is wholly too small to be used for retraining an accurate DNN from scratch). The post-training scenario is important because in practice the defender may not have access to the data set that was used to train the classifier/model. For example, the model may have been purchased by an entity (e.g. a company or government), without any “data rights” allowing access to the training set that was used. Moreover, if the model was built long ago (a legacy system), the training set may be lost or inaccessible.

[17, 3] attempt to cleanse the training set, while Fine-Pruning [11] and I-BAU [26] are both post-training mitigation approaches that refine the (presumed poisoned) model. These four methods are agnostic to the manner of backdoor incorporation. Neural Cleanse (NC) [19] is a post-training, reverse-engineering based detector that assumes the backdoor pattern is incorporated into a sample via a “blending” operation (with patch-replacement a special case of blending). [19] also proposed a method to mitigate the poisoned model, informed by the reverse-engineered (estimated) backdoor trigger.

In this paper, we focus on a reverse-engineering (inversion) based defense, which can be used to: detect whether or not a model was backdoor-poisoned (and, if so, identify its target class), to cleanse the training set, e.g., [17, 3], and for test-time backdoor-trigger detection. Moreover, reverse-engineering defenses are fundamental to explainable/interpretable AI – they identify a (malicious or suspicious) “cause” (the trigger pattern) for why the model is making a particular (perhaps peculiar) decision on a given test sample. A weakness

in some existing reverse-engineering defenses is that they may fail when the backdoor incorporation mechanism assumed by the defense (e.g., additive) does not match the mechanism actually used by an attacker (e.g., blending). This work remedies this weakness, developing a post-training detector that reverse-engineers the backdoor pattern while, at the same time, being *agnostic* to the method of backdoor pattern incorporation. Our attack-defense experiments, focused on the image classification domain, demonstrate that this approach, with minimal assumptions, achieves strong performance (a distinctive detection signal) across a variety of backdoor attacks with different incorporation methods.

## 2 Prior work on agnostic backdoor defenses

Though not all post-training, backdoor detection defenses are reverse-engineering based, e.g., [11, 25, 20], several reverse-engineering defenses have been proposed, e.g., [19, 12, 24], all relying upon a small, clean (unpoisoned, correctly labeled) dataset (which may be disjoint from the training set of the DNN under consideration).

[24] leverages a small, clean dataset to reverse-engineer putative backdoor patterns. This is achieved by seeking the smallest common additive perturbation that induces most patterns from one class (a putative source class) to be misclassified to another class (a putative target class). The common additive perturbation is *either* estimated at the input layer or in an internal (embedded) layer of the DNN. Working on an embedded layer is motivated by cases where the input space is discrete-valued (hence unsuitable for gradient-based estimation of perturbations) or when the embedded feature dimension is much smaller than the input dimension, e.g. for a Video Transformer model. A backdoor pattern estimated in an embedded space can be mapped back to the input space for purposes of interpretation using methods such as Grad-CAM [15]. It was also demonstrated in [24] (but in a quite limited way) that estimating an *additive* backdoor pattern in an embedded feature space of the DNN is *somewhat* agnostic to the method of backdoor incorporation – a multiplicatively incorporated backdoor was detected working from an internal layer of the DNN. However, other non-additive backdoor-incorporation mechanisms were not investigated in [24].

UNICORN [22, 23] is a reverse-engineering detector that attempts to be agnostic to the backdoor-incorporation mechanism. Considering only all-to-one backdoor attacks, two (unpoisoned) UNet feature maps (neural networks) are assumed available for each (putative target) class in order to produce, from the model’s input space, a feature space within which the backdoor pattern (hopefully) expresses either as a (BadNet) patch [5] or as a (Neural Cleanse - NC) blended patch [19], see equation (4) of [23]. So, generally, UNICORN’s design thus either requires assuming suitable unpoisoned feature maps are available or substantial computation to train them using unpoisoned data, the latter particularly when the number of classes is large, **before** the backdoor reverse-engineering process (NC) can commence. Moreover, if the attack is instead one-to-one, these methods may need to train two UNets for every putative

(source,target) class pair, which would entail huge computation even for a small number of classes (e.g., for 10 classes there are 90 class pairs).

Note that, in principle, one could form an ensemble of reverse-engineering based detectors, with each such detector assuming a particular method of backdoor incorporation. However, for “digital” attacks (as discussed before), there are effectively an *uncountably infinite number* of possible backdoor incorporation mechanisms. Even covering a substantial number of the possible mechanisms would entail an ensemble system of very high complexity (both with respect to detector design as well as detection inference complexity), while still failing to cover myriad possible mechanisms.

A backdoor-agnostic approach that is not reverse-engineering based is [20]. This work hypothesizes and experimentally verifies that backdoor-poisoned DNNs *overfit* to the backdoor pattern. Such overfitting is necessary in order for the backdoor’s features to overcome the “normal” source-class discriminative features, which would otherwise ensure classification to the (true) source class of the sample. Overfitting to the backdoor pattern implies that the backdoor pattern triggers large internal-layer DNN signals, which are particularly enabled by (positively) unbounded ReLU activations. [20] also demonstrated that optimizing saturation (clipping) levels on the ReLUs is effective at eliminating the backdoor mechanism from the trained model. However, [20] does not reverse-engineer the backdoor pattern.

Another important aspect is that, whereas for some backdoor attacks the backdoor pattern is a *static* pattern (e.g., the same pattern *added* to every poisoned training image) for other attacks, the backdoor pattern is effectively *sample-dependent*. The backdoor pattern induces sample-dependent *changes* both in the case of the warping attack [14] *as well as* in the case of patch replacement attacks (which, e.g. for digital images, involve replacing the pixel intensities in the backdoor patch region by the intensities of the backdoor patch).

The backdoor detector CEPA proposed herein has several key characteristics, exploiting some ideas from prior works: i) it estimates the backdoor pattern like [19, 24, 23] and unlike [20]; ii) it attempts to identify an **embedded** (internal layer) additive consensus perturbation that corresponds to the backdoor, like [24]<sup>2</sup>; iii) it exploits the observation from [20] that the trained model overfits to the backdoor pattern, with this overfitting achieved by the backdoor eliciting large internal-layer signals in the DNN; iv) like [26], it estimates *sample-specific*, backdoor mechanism-agnostic perturbations (thus enabling detection of backdoor attacks that involve sample-dependent changes such as patch replacement [5] or warping [14]). While the backdoor pattern may cause sample-dependent changes (i.e., at the input to the DNN), these sample-dependent changes may be inducing a very similar (i.e.,  $\sim$  a *common*) pattern in some layer of the DNN, i.e., a pattern that the network can learn to recognize (and which induces the model to misclassify to the attacker’s target class). Thus, we seek a *common* (consensus) backdoor pattern, not in the input sample, but in internal layer features of the

---

<sup>2</sup>This hypothesis of additivity in the embedded feature space is motivated by the observation that components of embedded feature-maps of a DNN are typically weighted and *superposed* in subsequent processing by, e.g., convolutional or linear layers.

DNN that are induced by input samples. Moreover, consistent with the backdoor overfitting phenomenon [20], this common backdoor pattern should express as a *large* internal-layer perturbation (even though the *input* perturbation may be small in magnitude in order to be inconspicuous).

### 3 Proposed Backdoor Detection Method: CEPA

Let  $p_t(x)$  be the DNN’s class posterior probability of belonging to class  $t$ , given input sample  $x$  (obtained by using a softmax activation in the output layer of the network). The classifier uses a winner-take-all-rule, i.e. the decided class is  $\hat{c}(x) = \arg \max_k p_k(x)$ . Furthermore, given the feedforward DNN structure, the class posterior can be expressed as:

$$p_t(x) = g_t(f(x))$$

where  $f(x)$  is the output of some internal layer of the DNN, i.e., it is an embedded feature vector activated by input sample  $x$ .

For each putative backdoor target class  $t$  or, when considering one-to-one attacks, each putative backdoor target class  $t$  paired with a putative source class  $s \neq t$ , we formulate an optimization problem, seeking sample-wise input perturbations ( $\delta_x$ ) which: 1) induce misclassification to the putative target class  $t$ ; 2) are inconspicuous (small); and 3)  $\sim$  induce a *common* perturbation of the embedded feature vector  $f(\cdot)$  (which is a putative backdoor pattern). A backdoor detection can then be made if: 1) the induced embedded feature vector perturbations have small variation about their mean ( $\mu$ ) (with this mean treated as the common backdoor pattern in the embedded space) and 2) the common perturbation  $\mu$  has unusually *large* magnitude (consistent with the backdoor overfitting phenomenon observed in [20]). Likewise, for class pairs  $(s, t)$  that are *not* involved in a backdoor attack, we expect that the estimated input perturbations  $\delta_x$  will essentially amount to *adversarial perturbations* (associated with adversarial inputs, i.e. test-time evasion attacks, e.g. [2]). For successful TTE attacks on two different input samples  $x$  and  $x'$  from the same class, there is *no* expectation that they will induce a *common* perturbation  $\mu$  in the embedded space, i.e. we would expect that the variance about  $\mu$  in the embedded space will be high for non-backdoor class pairs. Moreover, for such pairs, since there is no backdoor mapping, there will be no “backdoor overfitting”, i.e. we would expect that for such pairs  $\|\mu\|$  will be small compared to that for the backdoor class pair.

Accordingly, specialized for one-to-one attacks, for a given (source, target) class pair  $(s, t)$ , we define the objective function to be minimized over the sample-wise input perturbations  $\delta_x$  and the common embedded perturbation  $\mu$ :

$$\frac{1}{|\mathcal{D}_s|} \sum_{x \in \mathcal{D}_s} \left( -\log p_t(x + \delta_x) + \lambda \|f(x + \delta_x) - f(x) - \mu\|^2 \right), \quad (1)$$

where  $\mathcal{D}_s$  is the set of clean samples originating from class  $s$ ,  $\lambda > 0$ , and the second term is the variance about the common embedded perturbation ( $\mu$ )<sup>3</sup>. This objective function is minimized by a two-step iteration: 1) gradient descent steps taken w.r.t.  $\delta_x \forall x \in \mathcal{D}_s$  and 2) closed-form update of  $\mu$ , noting that, given the input perturbations fixed, the globally optimal  $\mu$  is:

$$\mu_{s,t} = \frac{1}{|\mathcal{D}_s|} \sum_{x \in \mathcal{D}_s} (f(x + \delta_x) - f(x)). \quad (2)$$

Moreover, after each gradient descent step,  $\delta_x$  is "clipped" so that  $x + \delta_x$  is feasible, e.g., so that each element of  $x + \delta_x$  is in  $[0, 1]$  for the case of normalized pixel intensities. While we could explicitly penalize the sizes  $\|\delta_x\|$  in (1), these sizes are *implicitly* minimized by initializing them to zero vectors and terminating the optimization as soon as a sufficient fraction of source-class samples are misclassified to the target class (e.g., 90% of them).

After the optimization is performed for all candidate class pairs  $(s, t)$ , a backdoor detection is made if there is a class pair  $(s, t)$  with: 1) unusually small variance about the common embedded perturbation ( $\mu_{s,t}$ ) and 2) unusually *large*  $\|\mu_{s,t}\|$ . A single "consensus" detection statistic for each  $(s, t)$  can be formed, e.g. as the *ratio*:

$$\frac{\sigma_{s,t}}{\|\mu_{s,t}\|} := \frac{\sqrt{\frac{1}{|\mathcal{D}_s|} \sum_{x \in \mathcal{D}_s} \|f(x + \delta_x) - f(x) - \mu_{s,t}\|^2}}{\|\mu_{s,t}\|},$$

which should be unusually small for a backdoor (source, target) class pair compared with non-backdoor pairs. Detection inference can then be based either on MAD [19] or on order-statistic p-values [24], assessed using a null model that is estimated using all (source, target)  $((s, t))$  class pair detection statistics.

### 3.1 Discussion: Hyperparameters

One might consider the choice of the internal layer  $f(\cdot)$  and the Lagrange multiplier  $\lambda$  to be hyperparameters of our detector. However, our detection approach can be simultaneously applied to *various* layers of the DNN, with detection inference then based *only* on the layer with the *most extreme* detection statistic (smallest p-value). Thus, the internal layer can be chosen in an automated fashion (and is not really a hyperparameter of the algorithm). Similarly, as discussed next in the experiments section,  $\lambda$  can *also* be automatically adjusted, and is thus also not truly a hyperparameter of the algorithm. The threshold on the misclassification rate (used to terminate the CEPA optimization) is a hyperparameter of the algorithm. However, we have found experimentally that CEPA's performance is largely insensitive to the choice of this threshold.

<sup>3</sup>For all-to-one attacks, replace  $\mathcal{D}_s$  by  $\cup_{s \neq t} \mathcal{D}_s$  in (1), and the following  $\mu, \sigma$  quantities will be indexed by (i.e., depend on) just  $t$ , not  $s$  and  $t$ .

## 4 Experimental Results

### 4.1 Experiment Setup

**Datasets:** Our experiments are conducted on the benchmark datasets CIFAR-10 and CIFAR-100 [10]. CIFAR-10 contains 60,000  $32 \times 32$  color images from 10 classes, with 5,000 images per class for training and 1,000 images per class for testing. CIFAR-100 contains 60,000  $32 \times 32$  color images from 100 classes, with 500 images per class for training and 100 images per class for testing.

**Attack Settings:** On CIFAR-10, we consider the following triggers: 1) a  $3 \times 3$  random patch (**BadNet**) with a randomly selected location (fixed for all triggered images for each attack), used in [6]; 2) an additive perturbation (with size  $2/255$ ) resembling a chessboard [24]; 3) a warping-based trigger (WaNet) proposed by [14]; 4) a Hello Kitty trigger with a blend ratio of  $\alpha = 0.15$  used by [4]. We mainly considered all-to-one attacks, and arbitrarily chose class 9 as the target class. We set the poisoning rate at 1.8%. That is, we embedded the backdoor triggers in 100 randomly chosen training samples per class (excluding the target class). Moreover, to achieve similarly effective attacks as for other triggers, we poisoned 900 images per source class in the all-to-one attack for WaNet. Our CIFAR-100 experiment illustrates the scalability of CEPA. On CIFAR-100 we only consider the BadNet attack.

**Training Settings:** We trained a ResNet-18 ([7]) on CIFAR-10 and a VGG-16 ([16]) on CIFAR-100 for 30 epochs with a batch size of 32. For all attacks, we used the Adam optimizer ([9]) for parameter learning and a scheduler to decay the learning rate of each parameter group by 0.1 every 10 epochs. The initial learning rate was set to 0.01.

**Defense Settings:** For trigger estimation, we randomly selected 10 images per class from the test set to form the small clean dataset possessed by the defender. The remaining test instances were reserved for performance evaluation. For each putative target class, the parameter  $\lambda$  of (1) was initially set to 0.01 and dynamically adjusted based on the misclassification rate: If it is higher than 90% for 5 consecutive iterations,  $\lambda$  is increased by a factor of 1.5 (tightening the embedded consensus around the current  $\mu$ ). If it is lower than 90% for 5 consecutive iterations,  $\lambda$  is decreased by a factor of 1.5. The minimization of (1) is terminated when the mean norm of the  $\delta$ s ( $|\mathcal{D}_{-t}|^{-1} \sum_{x \in \mathcal{D}_{-t}} \|\delta_x\|$  where  $\mathcal{D}_{-t} = \cup_{s \neq t} \mathcal{D}_s$ ) did not decrease over 50 consecutive iterations while the misclassification rate is maintained over 90%.

### 4.2 Backdoor Detection Performance

Acting on layer 5 of the ResNet18 model, Figures 1 and 2 respectively show the performance of our defense in terms of the consensus measure consisting of the estimated standard deviation divided by the L2 norm of  $\mu$ ,  $\sigma/\|\mu\|$ , and in terms of  $\|\mu\|$ , on the four poisoned models and on an unattacked (clean) model. Figures 3 and 4 show the same measures for layer 13. From the bar charts (one bar for each *putative* target class), one can see that, for both layers 5 and 13,



Table 1: For each DNN layer and detection criterion, CEPA MAD statistics for the attacks against ResNet-18/CIFAR-10, and also for the Clean (unpoisoned) model.

Layer and criterion	BadNet	WaNet	Chessboard	Blend	Clean
5, L2 norm of $\ \mu\ $	27.47	7.11	7.48	7.25	0.50
5, consensus ( $\sigma/\ \mu\ $ )	2.54	4.12	5.72	2.25	0.23
13, L2 norm of $\ \mu\ $	9.13	4.10	0.23	3.91	0.75
13, consensus ( $\sigma/\ \mu\ $ )	3.58	2.72	0.34	1.71	2.02

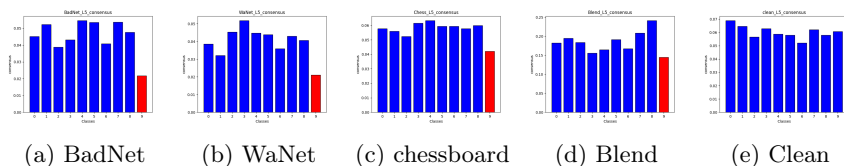


Figure 1: Layer-5 consensus,  $\sigma/\|\mu\|$

our method strongly indicates the true target class (9) on poisoned models, i.e., the quantities for the true target class are clear outliers with respect to those for the non-target classes (0-8)<sup>4</sup>, but does not indicate any significant outliers in the case of a clean model (i.e., there are no false positive class detections). The exception is the global chessboard backdoor, which is only clearly detected using layer 5. We again note that our method can be applied to a *plurality* of layers (embedded feature representations) of the model to detect backdoor poisoning.

Table 1 shows CEPA detection’s MAD statistics, e.g., [19]<sup>5</sup>. Note that the chessboard pattern is not detected (i.e.,  $MAD < 2$ , where 2 is the traditional detection threshold corresponding to two standard deviations beyond the median) using layer 13 with both L2 norm of  $\mu$  and consensus, but is detected at layer 5. Also, the clean model is “borderline” detected at layer 13 but not detected at layer 5. Again, CEPA can be run using a plurality of layers and both criteria, with a detection made, e.g., if any corresponding MAD in a range  $\geq 2$ . The MAD anomaly scores for all classes and all attacks are based on the data shown in Figures 1, 2, 3, and 4. Also from these bar charts (one bar for each *putative* target class), one can see that, for both layers 5 and 13, CEPA strongly indicates the true target class (9) on poisoned models, i.e., the quantities for the true target class are clear outliers with respect those for the non-target classes (0-8), but does not indicate any significant outliers in the case of a clean model (i.e., there are no false positive class detections). The exception is the global chessboard backdoor, which is only clearly detected using layer 5.

Some prior work on backdoor detection has suggested the use of cosine

<sup>4</sup>Such outlier detection is directly accomplished by applying, e.g., Median Absolute Deviation (MAD), on the null formed by the bar chart, as used in Neural Cleanse [19].

<sup>5</sup>Order-statistic p-values could be used instead of MAD, e.g., [24].

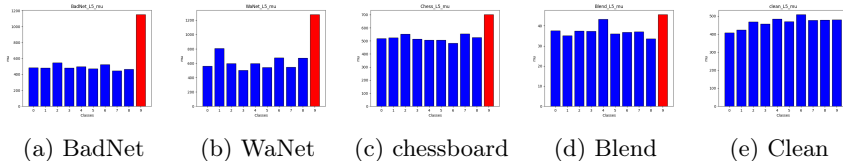


Figure 2: Layer-5 L2 norm of  $\mu$ ,  $\|\mu\|$

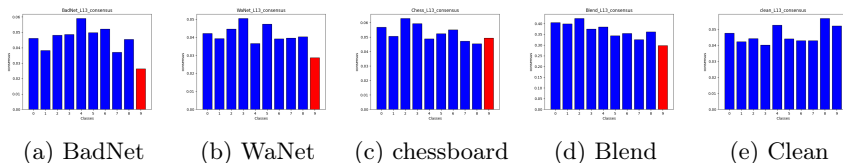


Figure 3: Layer-13 consensus,  $\sigma/\|\mu\|$

similarity as a detection statistic, e.g., [21]. In Figure 6, we plot the mean (pairwise) cosine similarity of the optimizing  $\delta$ s obtained from our method for each putative target class. Though the mean cosine similarity is relatively larger for the backdoor target class for chessboard than for BadNet (chessboard is an additive perturbation (which is not sample-specific), while BadNet’s patch is sample-specific because it involves replacing the portion of the image in the backdoor mask), the mean cosine similarity is not effective as a detection statistic, for either of the two attacks – this shows that  $\|\mu\|$  and the consensus measure  $\sigma/\|\mu\|$  (inspired by the backdoor overfitting phenomenon recognized in [20]) are quite distinctive as (sound) backdoor detection statistics.

In Table 2, attack success rates (ASRs) are evaluated on the test set when the ground-truth backdoor pattern is added to the test samples and when, instead, the perturbations obtained via (3) are added to test samples. Specifically, for evaluation, we

- randomly chose 100 correctly classified samples per source class from the CIFAR-10 test dataset,

ASR	BadNet	Blend	WaNet	chessboard
GT	95.73%	91.53%	97.31%	96.85%
(1)	92.22%	93.33%	96.67%	91.11%
(3)	91.11%	88.89%	81.11%	93.33%

Table 2: Attack success rates (for a 1.8% poisoning fraction of the training set) when: i) the ground-truth (GT) backdoor pattern is incorporated into the evaluation samples; ii) perturbations  $\delta$  obtained from (1) are incorporated into the samples of the small clean dataset  $\mathcal{D}$  use for defense; and iii) perturbations  $\delta$  obtained via (3) (given  $\mu$  from (1)) are incorporated into the evaluation set.

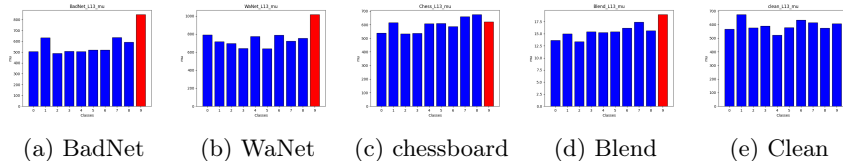


Figure 4: Layer-13 L2 norm of  $\mu$ ,  $\|\mu\|$

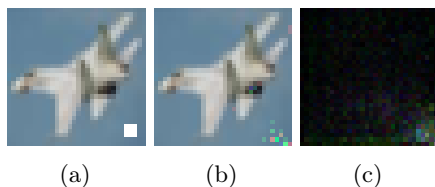


Figure 5: For the BadNet attack: (a) an image  $x$  with the ground truth trigger, (b) an image  $x$  with its estimated trigger  $\hat{\delta}_x$ , (c)  $|\mathcal{D}|^{-1} \sum_{x \in \mathcal{D}} \hat{\delta}_x$  with pixel intensities amplified by 5 for visualization.

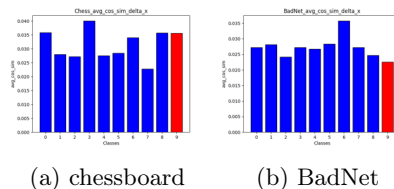


Figure 6: Mean pairwise cosine similarity of the optimizing  $\delta$ s.

- computed the input perturbation corresponding to a *given*  $\mu$  for a test sample  $x$  by gradient-based means,

$$\hat{\delta}_x = \arg \min_{\delta} \|f(x + \delta) - (f(x) + \mu)\|^2 + v\|\delta\|^2, \quad (3)$$

where in fact we set  $v = 0$  ( $v > 0$  explicitly encourages finding small-norm perturbations).

- calculated the percentage of those samples which were then classified to the target class (9).

From Table 2, we see that, with the exception of chessboard, using reverse-engineered perturbations based on  $\mu$  (3) on evaluation examples results in high ASR but not as high as using either the ground-truth (GT) perturbations nor the reverse-engineered perturbations on the samples used by the defense to identify

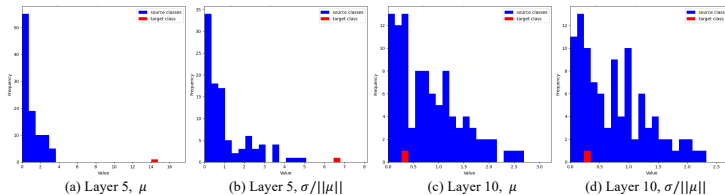


Figure 7: Histogram of MAD anomaly scores calculated on (a) L2 norm of  $\mu$  and (b) consensus in layer-5, (c) L2 norm of  $\mu$  and (d) consensus in layer-10.

$\mu$  (1). It is interesting that in one case (blend), the GT ASR is lower than that of (1).

While UNICORN [23] reports higher ASRs (see their Table 1), their poisoning fraction is 2.8 times higher (5%, see their Section A.5, compared to our 1.8%), which may make the backdoor pattern more conspicuous and more easily detected. Note, though, that a poisoning rate of just 1.8% is sufficient to achieve a very high attack success rate for the adversary (Table 2).

As mentioned above, if UNICORN’s feature maps are trained using the (possibly poisoned) training dataset of the defended model, then it is not truly a post-training defense. Again, the post-training backdoor detection scenario is important considering that, e.g., AIs are sometimes built from foundation models acquired from other parties or are produced by other parties and embedded in larger systems which are then acquired (with potentially no “data rights” access to the training set, for the party who purchases/acquires the model).

Additionally, CEPA

- truly possesses only a single hyperparameter (the misclassification fraction threshold, used to terminate the CEPA optimization), as the internal layer  $f(\cdot)$  and the parameter  $\lambda$  can be automatically chosen;
- does not involve a bound on the “size” of the backdoor pattern or its mask (unlike UNICORN’s “mask size constraint”) – indeed, it detects the chessboard pattern, which has global pixel support;
- demonstrates that auxiliary feature maps (as used by UNICORN) are not necessary and that the embedded features of the defended model suffice for achieving accurate agnostic backdoor detection.

CEPA has similarly good detection results and scalability on the 5th layer of VGG-16 model trained on CIFAR-100, as shown in Figure 7 against BadNet. More details are in Appendix A.

Also, see Appendix B for results of an adaptive BadNet attack on a ResNet-18 model designed for CIFAR-10.

### 4.3 Estimated Pattern Visualization and Analysis

**Visualizing Estimated Triggers.** In Figure 5, we visually compare the estimated backdoor pattern/trigger for the BadNet attack using CEPA with the ground-truth trigger: (a) is a clean image from class 0 (airplane) embedded with the ground truth trigger (lower right of the image); (b) is the same clean image embedded with the reverse-engineered ( $\delta_x$ ) trigger; and (c) is the average estimated  $\hat{\delta}$  over all clean samples of the source class,  $\mathcal{D}_s$ .

Note that, in CEPA’s loss function, triggers are (sample-wise) additively applied to images. The resulting, estimated sample-wise  $\delta_x$ ’s may in fact have non-zero values at all pixel locations (albeit small values at pixel locations that are *not* part of the ground-truth backdoor pattern’s support, for localized patch replacement attacks).

A notable observation from these visualizations is that, while there is discrepancy in appearance between the ground truth and the estimated learned triggers, they are in the same location.

#### 4.4 Time Complexity

Our experiments utilize an NVIDIA RTX 3090 GPU with 24GB of memory. CEPA requires approximately 2 hours to perform detection on a Resnet-18 model trained on CIFAR-10, using 10 clean images per class (90 images total). Conversely, detection on a VGG-16 model trained on CIFAR-100 using 2 clean images per class (198 images total) takes approximately 40 hours. For comparison, training a Resnet-18 on CIFAR-10 for 30 epochs takes approximately 20 minutes.

### 5 Summary and Discussion

This paper concerns post-training defense against backdoor poisoning in deep neural networks. The proposed method CEPA detects whether the model is backdoor poisoned and, if so, identifies the target class of the backdoor and also estimates the backdoor trigger pattern for a given sample. CEPA is agnostic to the manner of incorporation of the backdoor pattern (as well as agnostic to the backdoor pattern itself, of course). CEPA has low complexity and so is scalable (even when based on a plurality of embedded feature representations); requires few clean samples; requires very few hyperparameters (effectively, only a single one); relies only on embedded feature activations (not on auxiliary feature maps); and performs well, with our results easily reproduced by other parties. As noted earlier,  $\lambda$  can be dynamically adjusted during the optimization process, while different choices for the layer index of the embedded feature representation can be simultaneously assessed without large computational overhead.

### References

- [1] M. Belkin, D. Hsu, S. Ma, and S. Mandal. Reconciling modern machine-learning practice and the classical bias–variance trade-off. In *PNAS*, July 2019.
- [2] N. Carlini and D. Wagner. Towards Evaluating the Robustness of Neural Networks. In *Proc. IEEE Symposium on Security and Privacy*, 2017.
- [3] Bryant Chen, Wilka Carvalho, Nathalie Baracaldo, Heiko Ludwig, Benjamin Edwards, Taesung Lee, Ian M. Molloy, and Biplav Srivastava. Detecting Backdoor Attacks on Deep Neural Networks by Activation Clustering. In *AAAI*, 2019.
- [4] X. Chen, C Liu, Bo Li, Kimberly Lu, and Dawn Song. Targeted Backdoor Attacks on Deep Learning Systems Using Data Poisoning. *arXiv:1712.05526*, 2017.

- [5] T. Gu, K. Liu, B. Dolan-Gavitt, and S. Garg. BadNets: Evaluating Backdooring Attacks on Deep Neural Networks. *IEEE Access*, 7:47230–47244, 2019.
- [6] Tianyu Gu, Kang Liu, Brendan Dolan-Gavitt, and Siddharth Garg. BadNets: Evaluating Backdooring Attacks on Deep Neural Networks. *IEEE Access*, 2019.
- [7] Kaiming He, Xiangyu Zhang, Shaoqing Ren, and Jian Sun. Deep Residual Learning for Image Recognition. In *CVPR*, 2016.
- [8] Dan Hendrycks, Kevin Zhao, Steven Basart, Jacob Steinhardt, and Dawn Song. Natural adversarial examples. In *Proc. IEEE CVPR*, 2021.
- [9] Diederik P. Kingma and Jimmy Ba. Adam: A Method for Stochastic Optimization. In *ICLR*, 2015.
- [10] Alex Krizhevsky and Hinton. Learning multiple layers of features from tiny images. <http://www.cs.toronto.edu/~kriz/learning-features-2009-TR.pdf>, 2009.
- [11] K. Liu, B. Doan-Gavitt, and S. Garg. Fine-Pruning: Defending Against Backdoor Attacks on Deep Neural Networks. In *Proc. RAID*, 2018.
- [12] Yingqi Liu, Wen-Chuan Lee, Guanhong Tao, Shiqing Ma, Yousra Aafer, and Xiangyu Zhang. ABS: Scanning Neural Networks for Back-Doors by Artificial Brain Stimulation. In *Proceedings of the 2019 ACM SIGSAC Conference on Computer and Communications Security, CCS '19*, page 1265–1282, 2019.
- [13] S. Moosavi-Dezfooli, A. Fawzi, O. Fawzi, and P. Frossard. Universal adversarial perturbations. In *Proc. IEEE Conf. on Computer Vision and Pattern Recognition*, 2017.
- [14] Tuan Anh Nguyen and Anh Tuan Tran. WaNet - Imperceptible Warping-based Backdoor Attack. In *ICLR*, 2021.
- [15] S. Sattarzadeh, M. Sudhakar, K.N. Plataniotis, J. Jang, Y. Jeong, and H. Kim. Integrated Grad-CAM: Sensitivity-Aware Visual Explanation of Deep Convolutional Networks via Integrated Gradient-Based Scoring. <https://arxiv.org/abs/2102.07805>, 2021.
- [16] Karen Simonyan and Andrew Zisserman. Very Deep Convolutional Networks for Large-Scale Image Recognition. In *ICLR*, 2015.
- [17] Brandon Tran, Jerry Li, and Aleksander Madry. Spectral Signatures in Backdoor Attacks. In *NeurIPS*, 2018.
- [18] A. Turner, D. Tsipras, and A. Madry. Clean-label backdoor attacks. <http://people.csail.mit.edu/tsipras/pdfs/TTM18.pdf>, 2018.

- [19] B. Wang, Y. Yao, S. Shan, H. Li, B. Viswanath, H. Zheng, and B.Y. Zhao. Neural Cleanse: Identifying and Mitigating Backdoor Attacks in Neural Networks. In *Proc. IEEE Symposium on Security and Privacy*, May 2019.
- [20] H. Wang, Z. Xiang, D.J. Miller, and G. Kesidis. MM-BD: Post-Training Detection of Backdoor Attacks with Arbitrary Backdoor Pattern Types Using a Maximum Margin Statistic. In *Proc. IEEE Symposium on Security and Privacy*, 2024.
- [21] R. Wang, Gaoyuan Zhang, Sijia Liu, Pin-Yu Chen, Jinjun Xiong, and Meng Wang. Practical Detection of Trojan Neural Networks: Data-Limited and Data-Free Cases. In *Proc. ECCV*, 2020.
- [22] Z. Wang, K. Mei, H. Ding, J. Zhai, and S. Ma. Rethinking the Reverse-engineering of Trojan Triggers. In *Proc. NeurIPS*, 2022.
- [23] Z. Wang, K. Mei, J. Zhai, and S. Ma. UNICORN: A Unified Backdoor Trigger Inversion Framework. In *Proc. ICLR*, 2023.
- [24] Z. Xiang, D.J. Miller, and G. Kesidis. Detection of Backdoors in Trained Classifiers Without Access to the Training Set. *IEEE Transactions on Neural Networks and Learning Systems*, March 2022.
- [25] X. Xu, Q. Wang, H. Li, N. Borisov, C.A. Gunter, and B. Li. Detecting AI Trojans Using Meta Neural Analysis. <https://arxiv.org/abs/1910.03137>, Oct. 2019.
- [26] Y. Zeng, S. Chen, W. Park, Z. Mao, M. Jin, and R. Jia. Adversarial unlearning of backdoors via implicit hypergradient. In *Proc. ICLR*, 2021.
- [27] A. Zou, Z. Wang, J.Z. Kolter, and M. Fredrikson. Universal and Transferable Adversarial Attacks on Aligned Language Models. <https://arxiv.org/abs/2307.15043>, 2023.

## A BadNet against VGG-16 for CIFAR-100

VGG has fewer (fatter) layers than the comparable ResNet model, the layers selected to apply CEPA are more sensitive hyperparameters. Note that if we choose layers too close to the input, we don't get a suitable feature map for the embedded activation of the backdoor to manifest. Alternatively, if we choose a layer too close to the output, the target class "logit" signal dominates for the backdoor trigger.

In Table 3, we show CEPA detection's MAD statistics for the poisoned model. Both are  $> 2$ , i.e., the backdoor is successfully detected, at layer 5. Also, just as for the CIFAR-10 results in Table 1, there were no false positives for the clean/unpoisoned CIFAR-100 model.

Table 3: CEPA MAD statistics against BadNet on VGG-16/CIFAR-100

layer \ criterion	$\ \mu\ $	$\sigma/\ \mu\ $
5	28.44	14.03
10	0.52	0.51

## B Adaptive BadNet attack on ResNet-18 for CIFAR-10

Assume the attacker is the training authority and trains the model to minimize consensus (maximize variance of embedded perturbation corresponding to the backdoor). That is, for the poisoned training data subset  $\mathcal{X}_B$  of the training dataset  $\mathcal{X}$ , the training objective would be to minimize the cross-entropy loss over  $\mathcal{X}$  minus parameter  $\gamma > 0$  times the variance of the embedded perturbation of the ground-truth backdoor patterns in the poisoned training subset,  $(x + \delta_{B,x}, t) \in \mathcal{X}_B \subset \mathcal{X}$ :

$$\begin{aligned}
 & - \sum_{(x,y) \in \mathcal{X}} \log \hat{p}(y|x) \\
 & - \frac{\gamma}{|\mathcal{X}_B|} \sum_{(x+\delta_{B,x},t) \in \mathcal{X}_B} \|f(x + \delta_{B,x}) - f(x) - \mu_B\|^2,
 \end{aligned}$$

where

$$\mu_B = \frac{1}{|\mathcal{X}_B|} \sum_{(x+\delta_{B,x},t) \in \mathcal{X}_B} (f(x + \delta_{B,x}) - f(x)).$$

Based on the previous equation, we launched an adaptive attack on a Resnet-18 model trained on the CIFAR-10 dataset. The backdoor trigger was jointly optimized with the Resnet-18 model over 100 epochs, using a learning rate of 0.001. In one experiment, the adaptive attack parameter  $\gamma$  was set to 1 and the poisoning rate was 0.5 (50%). Consensus maximization for the adaptive attack was conducted in the penultimate layer of the Resnet-18 model. Under the adaptive attack, a high poisoning rate was needed to achieve a reasonable attack success rate (ASR), which in this case was 0.75. The clean-data accuracy (ACC) of the poisoned model was 0.83.

Subsequently, we implemented CEPA using the  $\|\mu\|$  criterion in the embedded feature space of the 5<sup>th</sup> layer of the poisoned Resnet-18 model. The backdoor was successfully detected with a MAD anomaly score of 46.36 for the true target class.